

Theoretical Studies on the Conformation of Protonated Dopamine in the Gas Phase and in Aqueous Solution

Peter I. Nagy,^{*,†} Giuliano Alagona,^{*,‡} and Caterina Ghio[‡]

Contribution from the Department of Medicinal and Biological Chemistry, The University of Toledo, Toledo, Ohio 43606-3390, and Istituto di Chimica Quantistica ed Energetica Molecolare del CNR, Via Risorgimento 35, I-56126 Pisa, Italy

Received May 4, 1998. Revised Manuscript Received March 23, 1999

Abstract: A trans (T) and two gauche (G1 and G2) conformers have been identified for protonated dopamine in the gas phase upon ab initio calculations up to the QCISD(T)/6-31G*//HF/6-31G* and MP2/6-311++G**//MP2/6-311++G** levels and based on B3LYP/6-31G* optimizations in DFT. Free energy differences at 298 K and 1 atm were calculated to be 3.2–5.6 kcal/mol between T and G1, and about 0 kcal/mol between the G2 and G1 conformers. The OH groups are nearly coplanar with the benzene ring and form an O–H···O–H intramolecular hydrogen bond in their most stable arrangement. Using the free energy perturbation method through Monte Carlo simulations, relative solvation free energies were evaluated in aqueous solution at $T = 310$ K and 1 atm. Ab initio/Monte Carlo torsional potential curves were calculated along pathways where small rotations about the C(ring)–C_β and C_β–C_α axes were allowed. No stable rotamers but the gas-phase optimized structures were identified. The T – G1 and G2 – G1 relative solvation free energies were calculated at -2.63 ± 0.31 and 1.34 ± 0.43 kcal/mol, respectively. The calculated T – G1 total free energy difference is at least 0.6 ± 0.3 kcal/mol in aqueous solution, predicting a G:T ratio of at least 75:25 as compared to the experimental value of 58:42. The calculated result is sensitive both to the applied basis set and to the level of the electron correlation considered upon obtaining the internal energy. When dopamine acts in a biological environment, its protonated form is presumably surrounded by counterions, mainly by chloride anions. If a chloride counterion, set at a N···Cl separation of 6 Å to estimate the upper bound of the counterion effect on a solvent separated DopH⁺ ion, is also considered in the solution simulations, the T – G1 relative solvation free energy takes a value of -0.55 ± 0.95 kcal/mol. Computer modeling shows that a close chloride ion largely modifies the solution structure in the immediate vicinity of protonated dopamine. The effect is different for the gauche and the trans conformers and leads to a decrease of the solvation preference for the trans form. Although the DopH⁺···Cl⁻ ion pair separated by a single water molecule is not favored in the bulk aqueous solution, such arrangement is possible in more restricted regions, e.g., in a receptor cavity or when passing lipid membranes. At such places one could expect an increase in the G conformer over the T form at pH = 7.4 and $T = 310$ K as compared to the G:T ratio found in D₂O solution of dopamine at pH = 7.

Introduction

It is generally accepted that some particular conformation of a biologically active molecule (ligand) at the receptor site is decisive in order to trigger a specific biological response.¹ Although the actual conformation is considerably affected by the interaction of the two parties, the ligand conformation is basically determined by its internal energy effects. This self-determination is more pronounced for charged ligands.

Dopamine is an important neurotransmitter. Its improper regulation is associated with neurological diseases such as Parkinsonism, where dopamine levels are reduced, and schizophrenia, which can be related to excess dopamine activity.² The biological significance of this molecule has drawn considerable theoretical and experimental interest for exploring its structure

in condensed phase.^{3–7} Conformational variety is possible due to rotations about a C–N and two C–C bonds. Structural differences may also be found due to changes in the intramolecular hydrogen bond pattern at the catecholic ring (Figure 1).

Dopamine is expected to exist in a neutral form in the gas phase. As a primary amine, it is protonated at the N-site in aqueous solution at pH below 8.³ Its protonation state, however, may be questioned in a biological environment. The idea that dopamine takes the protonated form in a living organism is based on the physiological pH = 7.4 for the blood. Since blood can be modeled basically as an aqueous solution, full hydration and prevalence of the protonated form may be expected with confidence throughout the transport process. More problems emerge when defining the solvation state of a ligand bound to a receptor. Water molecules identified by X-ray crystallography

[†] University of Toledo.

[‡] Istituto di Chimica Quantistica ed Energetica Molecolare del CNR.

(1) *3D QSAR in Drug Design*; Kubinyi, H., Ed.; ESCOM: Leiden, 1993.
 (2) See, e.g.: (a) Cooper, J. R.; Bloom, F. E.; Roth, R. H. *The Biochemical Basis of Neuropharmacology*; Oxford University Press: New York, 1986. (b) Birkmayer, W.; Riederer, P. *Understanding the Neurotransmitters: Key to the Workings of the Brain*; Springer-Verlag: New York, 1989. (c) Mathews, C. K.; Van Holde, K. E. *Biochemistry*; The Benjamin/Cummings Publishing Company, Inc.: Menlo Park, CA, 1996.

(3) Solmajer, P.; Kocjan, D.; Solmajer, T. *Z. Naturforsch.* **1983**, *38c*, 758.

(4) Urban, J. J.; Cramer, C. J.; Famini, G. R. *J. Am. Chem. Soc.* **1992**, *114*, 8226.

(5) Cramer, C. J.; Truhlar, D. G. *J. Am. Chem. Soc.* **1991**, *113*, 8305.

(6) Urban, J. J.; Cronin, C. W.; Roberts, R. R.; Famini, G. R. *J. Am. Chem. Soc.* **1997**, *119*, 12292.

(7) Alagona, G.; Ghio, C. *Chem. Phys.* **1996**, *204*, 239.

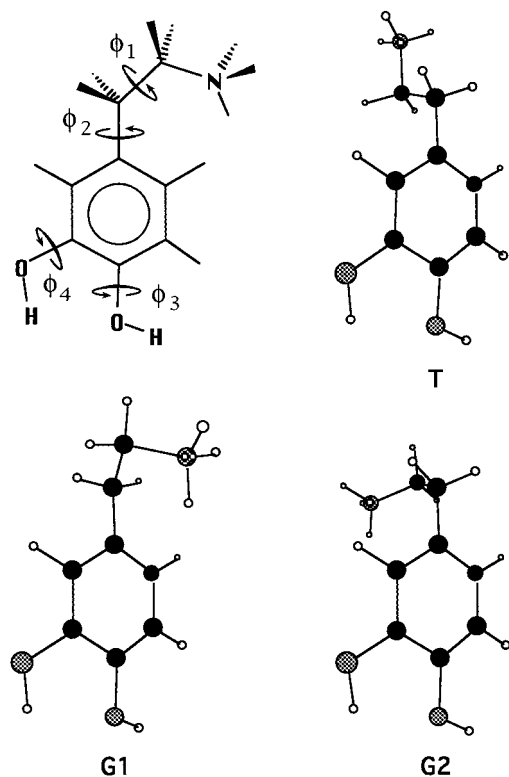


Figure 1. Definition of the ϕ_1 , ϕ_2 , ϕ_3 , and ϕ_4 torsional angles. All torsionals are zero on the schemes, counterclockwise rotations are taken as positive. Pairs of the optimized ϕ_1 , ϕ_2 values for the G1 (lower left), G2 (lower right), and T (upper right) conformers, respectively, are: HF/6-31G* (54.81, -112.40), (56.35, 80.17), (178.34, 98.60); MP2/6-31G* (54.62, -101.24), (55.41, 81.04), (178.67, 95.79); MP2/6-311++G** (49.01, -115.20), (51.32, 75.98), (178.75, 102.91); B3LYP/6-31G* (54.47, -104.75), (54.60, 85.03), (178.17, 99.52).

within the binding pocket of many proteins do not comprise a solution environment for the ligand. Methods used for obtaining structural and thermodynamic parameters for a solute molecule surrounded by an abundance of solvent molecules do not apply for a ligand partially solvated in the depth of a protein. Ligand binding on the receptor surface still cannot be modeled by a simple interaction of two molecules in solution. Even the determination of the acidic pK_a values for amino acid side chains in a protein presents a difficult computational problem.⁸

Since no dopamine receptor crystal structure is available at present, theoretical modeling about the ligand structure is even more important in this case. Our study aims at exploring the conformational equilibrium of protonated dopamine throughout the ligand transport process and at the onset of the interaction with the receptor system.

Solmajer et al.³ studied the conformational equilibrium for dopamine in D_2O by 1H NMR in the pH range of 2–11.5. They found the trans form (Figure 1) to be dominant at high pH, while the total gauche population is superior over the trans at low pH. Urban et al.⁴ performed theoretical calculations using the AM1-SM1 model⁵ for the neutral and ionized forms of dopamine. Important solvent effects on the conformational equilibrium were clearly indicated. In a recent project Urban et al.⁶ studied the conformational equilibria for several 2-phenethylamines, not including dopamine, at the MP2/6-311+G(d,p)//MP2/6-31G(d,p), as the highest level, in the gas phase, and using semiempirical continuum dielectric models for in-

solution calculations. The results suggest that the level of the ab initio calculations may be appropriate for calculating a subtle equilibrium, but the estimate of solvent effects requires a higher level approach. Alagona and Ghio⁷ calculated the conformational equilibrium for protonated dopamine in aqueous solution using the ab initio polarizable continuum model^{9a,b} and the HF/6-31G* basis set. Their results nicely reproduced the experimental finding by Solmajer et al.³

All of the calculations above represent studies where either the continuum solvent model was based on a semiempirical quantum chemical approach or the ab initio calculations used a relatively small basis set without considering electron correlation effects. Furthermore, no counterion effect can be considered within a continuum solvent approximation. Protonated dopamine in a biological system must be surrounded by counterions (mainly chloride) as well, which may affect the conformational equilibrium.^{10b}

The present study is in line with our previous work where the combined ab initio (gas phase)/Monte Carlo free energy perturbation calculations (solution) were compared with the results of the ab initio polarizable continuum model for the conformational equilibrium of 1,2-ethanediol,¹¹ 2-hydroxybenzoic acid,¹² and the diphenyl guanidinium ion.¹⁰ For the first time, however, a complete free energy potential curve has been calculated here for the protonated dopamine conformers along the perturbation pathways. The goal of these extended calculations was to explore whether there are stable conformers in the solution which are different from those found in the gas phase.

Methods and Calculations

Conformers were generated by rotations about the bonds indicated by the ϕ_1 , ϕ_2 , ϕ_3 , and ϕ_4 angles (Figure 1). Three main equilibrium structures T, G1, and G2 were considered, and many nonequilibrium geometries were calculated along the torsional pathways (Figure 2). All three conformers exist in pairs of mirror images. For computational ease the gauche conformers with positive ϕ_1 values were chosen. Several recent experimental studies on catechols¹³ indicate that neighboring OH groups on a benzene ring form an intramolecular hydrogen bond in their most stable arrangement in the gas phase. On the basis of our previous results,⁷ the geometry when the $O-H\cdots O-H$ moiety is coplanar with the benzene ring (as shown in Figure 1) has been generally chosen. For calculations with the $H-O\cdots O-H$ structure, see the next section.

Molecular geometries were obtained by optimization at the ab initio HF/6-31G* and MP2/6-311++G** levels (second-order Møller–Plesset electron correlation energy calculations^{14a–c} by means of the 6-311++G** basis set) and by means of the B3LYP functional in DFT

(9) (a) Miertus, S.; Scrocco, E.; Tomasi, J. *Chem. Phys.* **1981**, *55*, 117. (b) Tomasi, J.; Persico, M. *Chem. Rev.* **1994**, *94*, 2027. (c) Barone, V.; Cossi, M.; Tomasi, J. *Chem. Phys.* **1997**, *107*, 3210. (d) Olivares del Valle, F. J.; Tomasi, J. *Chem. Phys.* **1991**, *150*, 139.

(10) (a) Alagona, G.; Ghio, C.; Nagy, P. I.; Durant, G. J. *J. Phys. Chem.* **1994**, *98*, 5422. (b) Nagy, P. I.; Durant, G. J. *J. Chem. Phys.* **1996**, *104*, 1452.

(11) (a) Nagy, P. I.; Dunn, W. J., III; Alagona, G.; Ghio, C. *J. Am. Chem. Soc.* **1991**, *113*, 6719. (b) *Ibid.* **1992**, *114*, 4752. (c) Alagona, G.; Ghio, C. *J. Mol. Struct. (THEOCHEM)* **1992**, *256*, 187.

(12) (a) Nagy, P. I.; Dunn, W. J., III; Alagona, G.; Ghio, C. *J. Phys. Chem.* **1993**, *97*, 4628. (b) Alagona, G.; Ghio, C. *J. Mol. Liq.* **1994**, *61*, 1.

(13) (a) Burgi, T.; Leutwyler, S. *J. Chem. Phys.* **1994**, *101*, 8418. (b) Gerhards, M.; Perl, W.; Schumm, S.; Henrichs, U.; Jacoby, C.; Kleinemanns, K. *J. Chem. Phys.* **1996**, *104*, 9362. (c) Gerhards, M.; Perl, W.; Schumm, S.; Henrichs, U.; Kleinemanns, K. *Chem. Phys.* **1997**, *106*, 878.

(14) (a) Møller, C.; Plesset, M. S. *Phys. Rev.* **1934**, *46*, 618. (b) Pople, J. A.; Binkley, J. S.; Seeger, R. *Int. J. Quantum Chem.* **1976**, *10s*, 1. (c) Krishnan, R.; Frisch, M. J.; Pople, J. A. *J. Chem. Phys.* **1980**, *72*, 4244. (d) Lee, C.; Yang, W.; Parr, R. G. *Phys. Rev. B* **1988**, *37*, 785. (e) Becke, A. D. *J. Chem. Phys.* **1993**, *98*, 5648.

(8) (a) Warshel, A.; Sussman, F.; King, G. *Biochemistry* **1986**, *25*, 8368. (b) Bashford, D.; Karplus, M. *Biochemistry* **1990**, *29*, 10219.

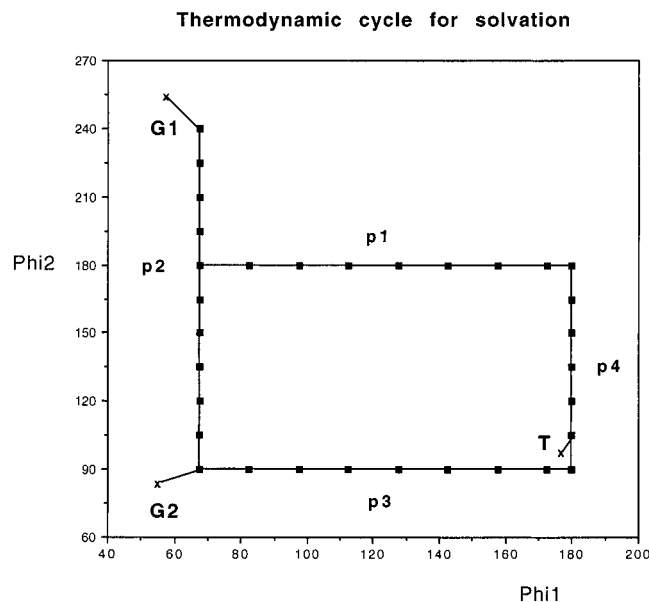


Figure 2. Pathways for calculating relative free energies in the gas phase and in aqueous solution.

Table 1. Relative Energy and Free Energy Results for Protonated Dopamine in the T, G1, and G2 Conformations^a

	T - G1	G2 - G1
HF/6-31G**/HF/6-31G*	3.53	-0.05
HF/6-311++G**/HF/6-31G*	3.67	0.14
MP2/6-31G**/HF/6-31G*	4.89	-0.21
MP3/6-31G**/HF/6-31G*	4.47	-0.15
MP4SDQ/6-31G**/HF/6-31G*	4.49	-0.11
QCISD/6-31G**/HF/6-31G*	4.42	-0.14
QCISD(T)/6-31G**/HF/6-31G*	4.56	-0.18
MP2/6-31G**/MP2/6-31G*	5.47	-0.32
MP2/6-311++G**/HF/6-31G*	5.41	0.08
MP2/6-311++G**/MP2/6-31G*	5.79	-0.14
MP2/6-311++G**/MP2/6-311++G**	5.84	0.11
B3LYP/6-31G**/B3LYP/6-31G*	4.43	-0.12
0.9ZPE + ΔH(0-298) - 298 ΔS(0-298) ^b	-0.29	0.23

^a Relative energy values in kcal/mol. ^b Vibrational frequencies computed at the HF/6-31G* level.

calculations.^{14d,e} Calculations were performed by the Gaussian 94¹⁵ running on the IBM RS6000/590 workstations at ICQEM. Geometry optimizations at the MP2/6-31G* level and several single-point calculations up to the QCISD(T) level¹⁶ were performed on the Cray Y-MP8 and T90 computers at the Ohio Supercomputer Center (Table 1). While imposing a planarity constraint on the benzene ring and connecting atoms, all other internal geometric coordinates were allowed to vary throughout optimizations for the T, G1, and G2 structures. The specific torsional angles were kept constant for calculating HF/6-31G* optimized geometries along the torsional pathways in Figure 2. Vibrational frequencies and thermodynamic parameters¹⁵ for the gas-phase structures were obtained at the HF/6-31G* level on a DEC2100 computer at CNUCE, the Pisa computing center. T, G1, and G2 turned out to be local energy minima. When structures along the torsional paths were compared, the vibrational frequency (generally imaginary) for the reaction coordinate was disregarded. The relative free energy

(15) *Gaussian 94, Revision D.4.* Frisch, M. J.; Trucks, G. W.; Schlegel, H. B.; Gill, P. M. W.; Johnson, B. G.; Robb, M. A.; Cheeseman, J. R.; Keith, T.; Petersson, G. A.; Montgomery, J. A.; Raghavachari, K.; Al-Laham, M. A.; Zakrzewski, V. G.; Ortiz, J. V.; Foresman, J. B.; Cioslowski, J.; Stefanov, B. B.; Nanayakkara, A.; Challacombe, M.; Peng, C. Y.; Ayala, P. Y.; Chen, W.; Wong, M. W.; Andres, J. L.; Replogle, E. S.; Gomperts, R.; Martin, R. L.; Fox, D. J.; Binkley, J. S.; Defrees, D. J.; Baker, J.; Stewart, J. P.; Head-Gordon, M.; Gonzalez, C.; Pople, J. A. *Gaussian, Inc.*: Pittsburgh, PA, 1995.

(16) Pople, J. A.; Head-Gordon, M.; Raghavachari, K. *J. Chem. Phys.* **1987**, *87*, 5968.

in the gas phase, $\Delta G(\text{gas})$ at $T = 298$ K and $p = 1$ atm, was calculated in the rigid-rotor, harmonic oscillator approximation¹⁷ as

$$\Delta G(\text{gas}) = \Delta G(298, 1\text{atm}) = \Delta E(0) + 0.9\Delta ZPE + \Delta\Delta H(0-298) - 298\Delta\Delta S(0-298) \quad (1)$$

Here $\Delta E(0)$ is the quantum mechanical energy difference and ΔZPE is the change in the vibrational energy at $T = 0$ K. A scaling factor of 0.9 was applied due to the overestimate of vibrational frequencies at the HF/6-31G* level.¹⁸ The terms $\Delta\Delta H(0-298)$ and $\Delta\Delta S(0-298)$ stand for the relative changes in enthalpy and entropy from $T = 0$ to 298 K.

For calculating the solvent effects, $\Delta G(\text{sol})$, the free energy perturbation method as implemented in Monte Carlo simulations¹⁹ and the polarizable continuum model (PCM,⁹ see its application for dopamine in ref 7) at the HF/6-31G*, B3LYP/6-31G*, MP2/6-31G**/HF/6-31G* and MP2/6-31G* levels were applied. Monte Carlo simulations in the NpT ensembles ($T = 310$ K, $p = 1$ atm) followed the procedure reported in previous works,^{10b,11a,b,12a} and as described originally by Jorgensen and co-workers.²⁰ The BOSS 3.6 program²¹ running on an SGI workstation at the University of Toledo was utilized, and steric parameters including those for united CH_x atoms ($x = 1, 2$), were taken from the program's library. The system consisted of an ion pair or a single cation and 496 TIP4P waters²² in a $24 \times 24 \times 24$ Å³ box with periodic boundary conditions. Intermolecular interactions were calculated by using the OPLS 12-6-1 potential.²³ Application of the ICUT = 2 cutoff option allowed consideration of extended solute-solvent atom-atom interactions with a maximum separation (SCUT) of 12 Å. The solvent-solvent cutoff radius (RCUT) was set to 8.5 Å. Preferential sampling was applied in order to enhance the speed of the convergence for the solution structure in the vicinity of the solute(s). The probability of selecting a solvent molecule for a move was proportional with $1/(R^2 + c)$, where R is the distance between the solvent oxygen and the reference point (C₁ atom) of the dopamine solute. The value of the c constant was set to 120. Solute and volume moves were attempted every 50 and 1000 steps, respectively. Simulations considered 3500 and 5000 K steps in the equilibration and averaging phases, respectively.

Monte Carlo simulations for the potential of mean forces (PMF) have been carried out for methylammonium chloride and for the DopH⁺...Cl⁻ (protonated dopamine with chloride counterion) ion pair with gauche and trans conformations for the DopH⁺ ion. Atomic charges for the cations were fitted to the HF/6-31G* electrostatic potential of the whole ion²⁴ using the CHELPG procedure.²⁵ PMFs were calculated upon changing the N...Cl distances in 0.2 Å increments within the 3-8 Å range. Using a double-wide sampling, free energy changes were calculated by the perturbation method with a step-size of ±0.1 Å. RCUT and SCUT were set as above, while the solute-solute interaction was fully considered throughout the whole PMF calculation. Long-range electrostatic effects (LRE) were considered to give a nearly constant energy contribution, because the cation geometry remained unaltered throughout the PMF simulation and because all atoms of the ion pair stayed, at any N...Cl separations, within a sphere with $R = 12$ Å, where the solvent molecules were explicitly considered.

(17) McQuarrie, D. *Statistical Mechanics*; Harper & Row: New York, 1976.

(18) Hehre, W. J.; Radom, L.; Schleyer, P. v. R.; Pople, J. A. *Ab Initio Molecular Orbital Theory*; Wiley: New York, 1986.

(19) Jorgensen, W. L.; Ravimohan, C. *J. Chem. Phys.* **1985**, *83*, 3050.

(20) (a) Jorgensen, W. L.; Madura, J. D. *J. Am. Chem. Soc.* **1983**, *105*, 1407. (b) Jorgensen, W. L.; Swenson, C. J. *J. Am. Chem. Soc.* **1985**, *107*, 1489. (c) Jorgensen, W. L.; Gao, J. J. *J. Phys. Chem.* **1986**, *90*, 2174.

(21) Jorgensen, W. L. BOSS, Version 3.6, *Biochemical and Organic Simulation System User's Manual*; Yale University: New Haven, CT, 1995.

(22) (a) Jorgensen, W. L.; Chandrasekhar, J.; Madura, J. D.; Impey, R. W.; Klein, M. L. *J. Chem. Phys.* **1983**, *79*, 926. (b) Jorgensen, W. L.; Madura, J. D. *Mol. Phys.* **1985**, *56*, 1381.

(23) Tirado-Rives, J.; Jorgensen, W. L. *J. Am. Chem. Soc.* **1988**, *110*, 1657.

(24) (a) Carlson, H. A.; Nguyen, T. B.; Orozco, M.; Jorgensen, W. L. *J. Comput. Chem.* **1993**, *14*, 1240. (b) Orozco, M.; Jorgensen, W. L.; Luque, F. J. *J. Comput. Chem.* **1993**, *14*, 1498.

(25) Breneman, C. M.; Wiberg, K. B. *J. Comput. Chem.* **1990**, *11*, 361.

Table 2. Atomic Charges for Monte Carlo Simulations (United CH_x Atoms), Obtained from CHELPG, as Compared to the AM1/CM2 Ones^a

	PG		PT		G1		G2		T		DopH ⁺		
	MeNH ₃ ⁺	AM1/	AM1/	AM1/	AM1/	AM1/	AM1/	AM1/	AM1/	AM1/	DopH ⁺		
	CHELPG	CM2	CM2	CM2	CM2	CM2	CM2	CM2	CM2	CM2	max	min	
C ₁ (ring)		0.044	-0.140	0.030	-0.113	0.148	-0.147	0.105	-0.145	0.061	-0.113	0.148	-0.001
C _β		0.071	0.124	0.010	0.090	0.014	0.128	0.059	0.129	0.028	0.090	0.098	-0.003
C _α	0.325	0.299	0.280	0.419	0.282	0.288	0.276	0.259	0.273	0.284	0.282	0.419	0.251
N	-0.288	-0.434	-0.678	-0.603	-0.684	-0.319	-0.676	-0.322	-0.676	-0.340	-0.684	-0.319	-0.603
H _{av}	0.321	0.328	0.425	0.375	0.423	0.292	0.425	0.295	0.425	0.312	0.424	0.380	0.229
q(NH ₃ ⁺)	0.675	0.549	0.596	0.522	0.587	0.555	0.598	0.563	0.600	0.597	0.587		

^a PG and PT values are charges used in calculations of the potentials of mean forces for the gauche and trans conformers in the DopH⁺···Cl⁻ dimers, respectively. Max and min values give the range for CHELPG atomic charges in DopH⁺ calculations.

Relative solvation free energies for the DopH⁺ conformers, either considering a chloride counterion or not, were calculated along the p1, p2, p3, p4 paths as shown in Figure 2. Atomic charges were fitted to the HF/6-31G* electrostatic potential of the ion in all reference conformations indicated in Figure 2 (Table 2). Relative solvation free energies were calculated using linear interpolation for geometric and potential parameters between reference points. Reference conformers differed in torsional angles by 15° at most, and 3–7 intermediate positions for the torsional angle were considered between.

When the MC calculations were completed, Li et al.²⁶ published a new method for calculating nonelectrostatic potential fitted atomic charges, named CM2. For comparison with the CHELPG values, the AM1/CM2 charges calculated by using the AMSOL 6.5.3 program²⁷ are also included in Table 2.

Long-range electrostatic effects on different DopH⁺ conformers were considered by using the Born equation for the free energy of hydration²⁸

$$G = -(q^2/2R)(1 - 1/D) \quad (2)$$

where q , R , and D are the atomic net charge, the effective ionic radius and the dielectric constant of the solvent, respectively. Equation 2 was applied for the sets of net atomic point charges immersed in a dielectric medium, and distributed as defined by the conformer geometry. Due to the cutoff procedure applied for the solute–solvent interaction (see above), each atomic center was surrounded by a sphere of explicitly considered solvent molecules. Long-range electrostatic interactions with the solvent were thus considered outside a sphere with an effective radius of $R = 12$ Å. The D value was taken as 53 for the TIP4P water model.²⁹ The sum of the G values from eq 2 for all atomic charges gives the G_{LRE} value for the specific conformer, in compliance with the generalized Born method.³⁰

An independent evaluation of the long-range electrostatic effects was carried out ab initio in the PCM framework. The corrections to the T – G1 and G2 – G1 free energy differences were calculated at the HF/6-31G*/HF/6-31G* level. A cavity made by a single sphere centered on the C₁(ring) atom was created around the solute with radius $R = 12$ or 16 Å. Effects of the out-of-sphere continuum dielectrics on the solute should thus correspond to upper and lower bounds of the true LRE values, respectively, if taking into consideration the molecular geometry, the SCUT value, and the ICUT procedure above. An intermediate case was considered when the cavity was formed by 14 interlocking spheres ($R = 12$ Å for each) centered on the atoms of the conserved catecholic part of the system and including the C_β atom.

(26) Li, J.; Zhu, T.; Cramer, C. J.; Truhlar, D. G. *J. Phys. Chem. A* **1998**, *102*, 1820.

(27) AMSOL 6.5.3. Hawkins, G. D.; Giesen, D. J.; Lynch, G. C.; Chambers, C. C.; Rossi, I.; Storer, J. W.; Li, J.; Zhu, T.; Rinaldi, D.; Liotard, D. A.; Cramer, C. J.; Truhlar, D. G. Department of Chemistry, University of Minnesota: Minneapolis, MN 55455-0431.

(28) Born, M. *Z. Phys.* **1920**, *1*, 45.

(29) (a) Neumann, M. *J. Chem. Phys.* **1986**, *85*, 1567. (b) Jorgensen, W. L.; Blake, J. F.; Buckner, J. K. *Chem. Phys.* **1989**, *129*, 193.

(30) See, e.g.: (a) Constanciel, R.; Contreras, R. *Theor. Chim. Acta* **1984**, *65*, 1. (b) Kozaki, T.; Morihashi, K.; Kikuchi, O. *J. Am. Chem. Soc.* **1989**, *111*, 1547. (c) Still, W. C.; Tempczyk, A.; Hawley, R. C.; Hendrickson, T. *J. Am. Chem. Soc.* **1990**, *112*, 6127. (d) Cremer, C. J.; Truhlar, D. G. *Science* **1992**, *256*, 213. (e) Hawkins, G. D.; Cremer, C. J.; Truhlar, D. G. *J. Phys. Chem.* **1996**, *100*, 19824.

Results and Discussion

Gas Phase. Results of the gas-phase calculations are summarized in Table 1. The calculated relative energy for the T and G1 conformers shows large sensitivity to the applied basis set and the level of theory. Using the HF/6-31G* optimized geometries, HF results obtained either with the 6-31G* or the 6-311++G** basis set predict 3.5–3.7 kcal/mol for the T – G1 energy difference. Considering electron correlation effects in a series of calculations from the MP2/6-31G* to the QCISD(T)/6-31G* level, the relative energy falls in the range 4.4–4.9 kcal/mol. The B3LYP/6-31G*/B3LYP/6-31G* calculations give a relative energy of 4.4 kcal/mol. At the MP2/6-311++G** level or in calculations taking the MP2/6-31G* optimized geometries the relative energy is always larger than 5 kcal/mol. In contrast, the G2 – G1 relative energies are fairly constant in most comparisons. Although the G2 energy was estimated to be somewhat higher than the G1 value in two cases, G2 was generally found to be more stable than G1 by up to 0.3 kcal/mol.

Calculations show a moderate sensitivity of the relative energies to the level of the geometry optimization. The MP2/6-31G*/MP2/6-31G* and MP2/6-31G*/HF/6-31G* values for the T – G1 energies differ by 0.58 kcal/mol. In the MP2/6-311++G** calculations an energy range of 0.43 kcal/mol has been obtained. The method of the geometry optimization has, however, only a small effect on the G2 – G1 energy difference. In general, our previous finding,³¹ that the level of the single point calculations rather than the method used in obtaining optimized geometries affects the relative conformer energies, has been confirmed here. Relative thermal corrections are small for the DopH⁺ conformers, but while they hardly affect the T – G1 energy difference and leave G1 much more stable than T according to any calculations, the relative free energy is about 0 kcal/mol for the G2/G1 pair, indicating nearly equal populations for the two gauche forms in the gas phase.

Optimized torsional angles (Figure 1) deviate generally by no more than 6–7°. The only remarkable exception was found for ϕ_2 in the G1 conformer where the two MP2 optimized values differ by 14°. It is worth mentioning that most HF/6-31G* values are between those obtained at the MP2 optimization levels or that the HF values are very close to one of them. This means that the HF/6-31G* optimization results in reliable geometry for the protonated dopamine conformers; thus, its use in finding the geometries at paths 1–4 (Figure 2) is reasonable. The B3LYP/6-31G* torsional angles are closest to the corresponding MP2/6-31G* optimized values.

As was emphasized in the conformational analysis for histamine³² and in a recent study for 2-phenethylamines,⁶ the

(31) Nagy, P. I.; Novak-Takacs, K. *J. Am. Chem. Soc.* **1997**, *119*, 4999.

(32) Nagy, P. I.; Durant, G. J.; Hoss, W. P.; Smith, D. A. *J. Am. Chem. Soc.* **1994**, *116*, 4899.

gauche conformation of the $X-CH_2-CH_2-NH_3^+$ side chain is favorable if X is an aromatic ring. The NH_3^+ group can preferably interact with the π -system of the ring. Optimized ϕ_2 values are sensitive to both the basis set and the level for the G1 conformer, indicating subtle effects in the NH_3^+ -ring interaction. Benzene ring is rotated by 180–190° for G1 as compared to that for G2. Although the position of the ring relative to the plane of the $C(\text{ring})-C_\beta(\text{chain})-C_\alpha(\text{chain})$ atoms is nearly the same, the different signs for ϕ_2 result in a location of the $O_{\text{m(eta)}}$ and NH_3^+ groups on the opposite sides of the C–C–C plane in G1, while the two groups are on the same side in G2. Energy results show only a slight preference for the G2 arrangement, presumably due to a stronger $NH\cdots O_{\text{m}}$ electrostatic interaction.

Overall, because of a possible π -interaction between the NH_3^+ group and an X aromatic ring in the $X-CH_2-CH_2-NH_3^+$ moiety, the gauche arrangements of the end groups are favored in this type of 1,2-disubstituted ethanes. The stabilization with respect to the extended trans form is about 4–6 kcal/mol, with imidazole,³² benzene,⁶ and *p*-OH and *p*-F benzene⁶ substituents in the X position. The numerical value depends on the sophistication of the ab initio calculations but is fairly constant at the MP2/6-311+G** and MP2/6-311++G** levels.

Solvent Effects. The charge set accepted in solution simulations is a central problem when using effective pair potentials. In the present Monte Carlo simulations the CHELPG charges were utilized (Table 2) in compliance with the results of Carlson et al.^{24a} and Orozco et al.,^{24b} who pointed out that electrostatic potential fitted charges are superior in comparison with Mulliken charges, and these charges provide reasonable calculated values for the free energy of hydration (see below).

The CHELPG atomic charges in the present study show remarkable dependence on the conformation. This finding raises the question whether this feature could be an artifact, while nonelectrostatic potential fitted charges may not be so sensitive to conformational changes. In fact, the AM1/CM2 charges²⁶ in Table 2 show larger stability upon rotations of the side chain. Comparing, however, the sum of some atomic charges, one finds that the CM2 charges are more positive only at most 0.07 units as compared to the CHELPG charges for the NH_3^+ group, and the difference in the total charge along the $CH_2-CH_2-NH_3^+$ moiety is only 0.05–0.15 units (with more positive values always with the CM2 set). The conformational dependence of the total charge for this chain is 0.04 units with CM2 charges, which value does not differ very much from the charge modification of 0.09 with the CHELPG charges. Thus, CHELPG provides sometimes large bond moments, as CM2 also produces, but the conformational dependence of the whole side chain is fairly damped with both sets.

In the case of an ionic species the overall neutrality requirement demands a counterion in the vicinity. In solution the ions may or may not be separated by solvent molecules. For bulky ions their conformations depend on their internal energy, their interactions with the solvent, and with other ions present in solution.

A theoretical study for the diphenyl guanidinium ion revealed that close acetate and chloride counterions have a remarkable effect on the conformational equilibrium.^{10b} For this reason, PMFs were calculated here and compared first for the $CH_3NH_3^+\cdots Cl^-$ and $DopH^+\cdots Cl^-$ ion pairs. A clear local minimum was found for $CH_3NH_3^+\cdots Cl^-$ at $R(N\cdots Cl) = 3.2 \text{ \AA}$ corresponding to the contact ion pair structure. Because of the finite cutoff applied for the solute–solvent interaction, however, more and more water molecules are considered in this interaction

when the $N\cdots Cl$ separation increases. This effect will produce an artificial stabilization at larger separations, where the Coulombic interaction of the solute ions is already diminished. In fact, the PMF decreases monotonically in the range of 4–8 Å without a proper asymptotic behavior. The $DopH^+\cdots Cl^-$ system with gauche $DopH^+$ exhibits a shallow local minimum at $R(N\cdots Cl)$ of 3.3–3.6 Å, but the $DopH^+$ ion in trans conformation is not even locally stabilized by a contact Cl^- ion. PMFs with $DopH^+$ were calculated at selected PG and PT conformations (see Table 2 and Figure 1) with torsional angles $\phi_1 = 67.5^\circ$, $\phi_2 = 180.0^\circ$, and $\phi_1 = 180.0^\circ$, $\phi_2 = 180.0^\circ$, respectively, thus the obtained results may not be considered of general validity. What the PMF results simply suggest is that the $DopH^+\cdots Cl^-$ system, in contrast to the $CH_3NH_3^+\cdots Cl^-$ ion pair, is not stable in contact ion pair arrangement and at least one water molecule is located between the ions.

When biological conditions are modeled, the solution concentration should fit accordingly. The isotonic saline solution is about 0.15 M for the total salt concentration. Assuming chloride as the inorganic anion, one Cl^- ion in a $24 \times 24 \times 24 \text{ \AA}^3$ box approaches closely the required concentration. Monte Carlo simulations with a counterion were performed at an $N\cdots Cl$ distance of 6 Å. This separation of the ion pair corresponds approximately to the closest solvent-separated arrangement. As concluded from the PMFs, a variable $N\cdots Cl$ separation would lead to a gradually increasing ion separation. Thus, the selected $N\cdots Cl$ distance and calculated relative free energy should reflect the *upper bound* of the solvent-separated counterion effect, and the calculations with the single $DopH^+$ ion would reflect the lower bound.

Figures in the Supporting Information (S1–S4) show the free energy profiles along the four paths of Figure 2. The calculation of the relative solvation free energies for the T to G1 and G1 to G2 transformations would not require path p3. It was found previously, however, that the theoretical requirement for a zero net change in a thermodynamic cycle may not be met with a step size not sufficiently small throughout the application of the free energy perturbation method.³³ Although an increased number of steps could produce the zero net energy change in the cycle, the calculated standard deviation will increase, however, leading to rather uncertain average value. For testing the adequacy of the step size, we calculated the change of the solvation free energy along the rectangle in Figure 2, and a value of $0.26 \pm 0.57 \text{ kcal/mol}$ was obtained. The small deviation from zero is within the standard deviation calculated for the whole cycle.

The total relative free energy in solution, ΔG_{sol} , was calculated as $\Delta G_{\text{sol}} = \Delta G(\text{gas}) + \Delta G(\text{solv})$, where the latter term stands for the relative solvation free energy calculated in the MC simulations. Along all paths the MP2/6-311++G**//HF/6-31G* $\Delta E(\text{gas})$ curves and the $\Delta G(\text{gas})$ curves, obtained by adding thermal corrections to $\Delta E(\text{gas})$, run very closely. (Curves in Figures S2 and S4 show points referring to the T, G1, and G2 structures as well. Their indicated values differ slightly, however, from the correct values given in Table 1. $\Delta G(\text{gas})$ of conformers along the paths do not contain contributions from the vibration corresponding to the reaction coordinate. Since the T, G1, and G2 geometries do not fit into any of paths 1–4, the $\Delta E(\text{gas})$ and $\Delta G(\text{gas})$ curves are broken at these points.)

Courses of the ΔG_{sol} curves (with contribution of the $\Delta G(\text{solv})$ term calculated *without* considering the counterion,

(33) Dunn, W. J., III; Nagy, P. I.; Collantes, E. R. *J. Am. Chem. Soc.* **1991**, *113*, 7898.

Table 3. Relative Energy and Free Energy Results from Solvent-Effect Calculations^a

	T - G1	G2 - G1
Monte Carlo		
$\Delta G(\text{solv})$		
without counterion	-2.22 ± 0.31	1.30 ± 0.43
with counterion	-0.14 ± 0.95	
long-range electrostatics		
generalized Born, $R = 12 \text{ \AA}$	-0.30	0.81
PCM single sphere, $R = 12 \text{ \AA}$	-0.41	0.04
PCM 14 spheres, $R = 12 \text{ \AA}$	-0.37	0.04
PCM single sphere, $R = 16 \text{ \AA}$	-0.15	0.02
ΔG_{sol} (MP2/6-311++G**)	2.49 ± 0.31	1.65 ± 0.43
ΔG_{sol} (MP2/6-311++G**//MP2/6-31G*)	2.87 ± 0.31	1.43 ± 0.43
ΔG_{sol} (HF/6-31G*)	0.61 ± 0.31	1.52 ± 0.43
continuum solvent ^b		
ΔG_{sol} (MP2/6-31G**//MP2/6-31G*)	-0.76	-0.56
E_{elst}	-5.75	-0.43
DCR	-0.18	-0.04
ΔG_{sol} (HF/6-31G*)	-1.41	0.59
EP_{su}	0.73	-0.22
$E_{\text{su}}/E_{\text{sv}}$	-5.18	0.65
E_{elst}	-4.45	0.43
DCR	-0.20	-0.02
ΔG_{sol} (B3LYP/6-31G**//B3LYP/6-31G*)	-1.50	-0.23
EP_{su}	0.67	-0.27
$E_{\text{su}}/E_{\text{sv}}$	-6.04	-0.05
E_{elst}	-5.38	-0.32
DCR	-0.25	-0.01

^a Energy terms in kcal/mol. Geometries optimized in the gas phase at the HF/6-31G* level unless other level indicated. ΔG_{sol} values were calculated without counterion for solvation. ^b EP_{su} : solute polarization; $E_{\text{su}}/E_{\text{sv}}$: polarized solute/solvent electrostatic interaction; DCR: sum of the dispersion, cavity, and repulsion energy terms.

Figures S1–S4) basically follow those of the $\Delta G(\text{gas})$ curves. (Solvent effects along the paths were calculated without considering the long-range electrostatic contribution, which hardly differs in two consecutive steps of the present FEP calculations. LRE correction was taken into account, however, when the equilibrium composition of the mixture of conformers was calculated, see Table 3.) Local and global minima appear at nearly the same torsional angles, but the barrier heights are reduced in solution. Using a common reference point ($\phi_1 = 180^\circ$, $\phi_2 = 180^\circ$) for all curves, the global ΔG_{sol} minimum of -4.28 kcal/mol appears for the G1 structure. Local minimum values are of -2.88 kcal/mol for G2 and -1.44 kcal/mol for T. A high-lying local minimum was found along path 1 at $\phi_1 = 82.5^\circ$, $\phi_2 = 180^\circ$, but its ΔG_{sol} value (+2.31 kcal/mol) is too unfavorable for letting the conformer appear in the equilibrium mixture. In summary, no low-energy conformation has been found in aqueous solution that would basically differ from the G1, G2, and T structures optimized in the gas phase. This is an important finding, because the assumption that the gas-phase optimized structures provide relevant geometries also in solution always imposes uncertainty on those calculations.

The counterion effect can be assessed by inspection of the $dG(\text{counter})$ curves in Figures S1–S4. These curves describe the course of ΔG_{sol} when $\Delta G(\text{solv})$ was calculated from simulations considering the counterion, as well. (For technical reasons the ΔG_{sol} curves in S figures are designated by $dG(\text{sol})$ and $dG(\text{counter})$, without and with consideration of the counterion, respectively.) A new, high-lying local minimum of -0.77 kcal/mol is encountered at $\phi_1 = 157.5^\circ$ along p1. Otherwise the $dG(\text{counter})$ curves run below and basically parallel to the $dG(\text{sol})$ curves along the p1, p2, and p4 paths. The $dG(\text{counter})$ values for G1 and T are -6.78 kcal/mol and -1.87 kcal/mol, respectively. The most important conclusion is that, considering the counterion effect, the T - G1 total free energy separation

increases to 4.91 kcal/mol from a ΔG_{sol} value of 2.84 kcal/mol or from a value of 2.49 kcal/mol, considering all vibrations and LRE correction for the T and G1 minimum energy structures (Tables 1 and 3). The total free energy for G2 relative to G1 is 1.65 kcal/mol in solution, as calculated using the solvation terms from simulations, LRE correction, and thermal correction for the single DopH⁺ ion.

Long-range electrostatic effects, when using the generalized Born (GB) formula,³⁰ were calculated to be -28.2, -28.5, and -27.4 kcal/mol for the G1, T, and G2 conformers, respectively. The HF/6-31G* electrostatic potential fitted atomic charges, in the CH_x ($x = 1, 2$) united-atom approximation, present most polarized bonds at the side chain in the T conformation, and the most polarized benzene ring in the G1 form. The two effects partially compensate for the T - G1 pair, leading to a relative value of -0.3 kcal/mol (Table 3). The side-chain charges are similar in the gauche conformers, but the consistently more polarized bonds in the benzene ring for G1 result in a stabilization of 0.8 kcal/mol relative to G2.

Since the above result seems to be too much based on the CHELPG charges, an independent calculation of the LRE effect was desirable. The PCM calculation at the HF/6-31G* level, considering a single sphere with radius $R = 12 \text{ \AA}$, predicted -0.41 kcal/mol for the T - G1 correction, in close agreement with the GB value. The G2 - G1 correction, however, was different and amounted to only 0.04 kcal/mol. Thus, while estimate for the T - G1 LRE correction may be rather reliable, the correction for the G2 - G1 free energy separation remains unresolved. This is, however, a less important question, provided the dominance of G1 over G2 according to any calculations (Table 3). The PCM value above can be considered as the *upper bound* for the LRE correction to the free energy T - G1 separation. In fact, T - G1 and G2 - G1 were calculated at -0.15 and 0.02 kcal/mol, respectively when taking the $R = 16 \text{ \AA}$ for the radius of the sphere, and -0.37 and 0.04 kcal/mol, respectively, when the cavity was formed by fourteen interlocking spheres ($R = 12 \text{ \AA}$ for each). Basis set or level effects do not seem to be important. STO-3G calculations produce LRE corrections of -0.43 and -0.15 kcal to the T - G1 values considering a single sphere of $R = 12$ and 16 \AA , respectively, and -0.39 kcal/mol with the interlocking spheres. The G2 - G1 difference was negligible in all cases. 6-311++G**//HF/6-31G* calculations using a single sphere with $R = 12 \text{ \AA}$ give -0.44/-0.42 kcal/mol for T - G1, and 0.04/0.03 kcal/mol for G2 - G1 at the HF/MP2 level, respectively. All of these results together suggest that it is advisable to perform this type of calculations when a reliable estimate of the LRE effects is needed.

Experimental results of Solmajer et al.³ predict the prevalence of the gauche conformers over the trans at pH = 7. The gauche fraction is 58% as compared to the trans conformer of 42%. Assuming only one gauche conformer with remarkable contribution to the equilibrium mixture (Monte Carlo results in Table 3 predict a G2:G1 ratio of about 1:13), the 58:42 ratio corresponds to 0.19 kcal/mol relative free energy for the trans form at the experimental temperature of 296 K. The value is much smaller than our calculated value of 2.49 kcal/mol with MP2/6-311++G**//HF/6-31G* relative internal free energy and without considering counterion effects in solution. Inclusion of this latter effect would increase the T - G1 free energy separation by another 2 kcal/mol (relative solvation free energy is then only -0.14 ± 0.95 kcal/mol as compared to -2.22 ± 0.31 kcal/mol calculated without the counterion, Table 3). On the basis of the theoretical results one may conclude that the

Pair-energy distributions for ions

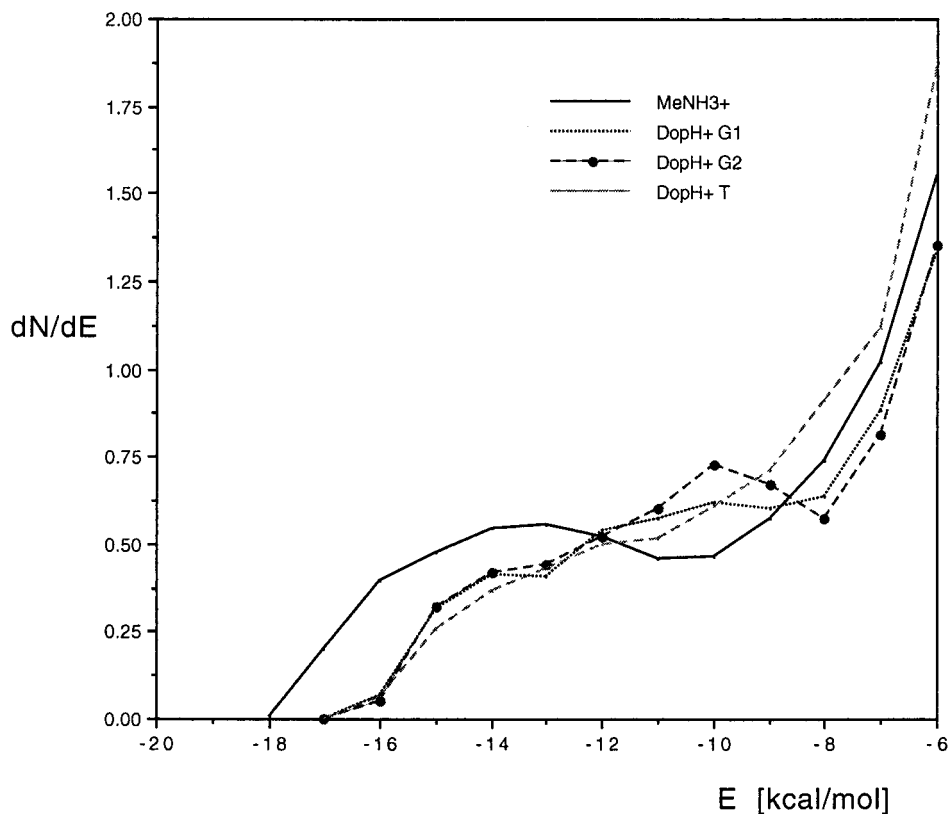


Figure 3. Pair-energy distributions for the MeNH_3^+ ion and for G1, G2, T conformers of the DopH^+ ion in aqueous solution.

solvent-separated counterion largely stabilizes the G1 conformer over the T form. On the basis of the experimental results (and predictions from the PMFs), however, close location of the Cl^- ion relative to the DopH^+ ion is energetically unfavored in the bulk of the aqueous solution, e.g., in blood throughout the transport process. Within a more restricted region such as a receptor cavity with a limited number of water molecules or when passing membranes, a closely located counterion could, however, affect the conformational equilibrium.

In contrast to those above, theoretical and experimental results are fairly close if considering the Monte Carlo ΔG_{sol} (HF/6-31G*) results in Table 3. HF/6-31G* results confirm that the counterion effect should be disregarded in bulk aqueous solution in order to get reasonable agreement with the experiment. Since no relevant conformations but the gas-phase optimized structures were found in solution, the equilibrium composition was calculated accordingly. The relative total free energy in solution for the T – G1 and G2 – G1 pairs are 0.61 ± 0.31 and 1.52 ± 0.43 kcal/mol, respectively, leading to G1:G2:T = 70:5:25 ratio at the experimental temperature of 296 K, and to a slightly modified composition of 68:6:26 at the computational temperature of 310 K, relevant for the human organism.

The deviation of the theoretical G:T ratio from the experimental one is due to the overestimation of the total relative free energy by about 0.4 kcal/mol. This value still reflects a state of the art result, but equilibria around the 50–50% composition are sensitive to changes in ΔG even by 0.1–0.2 kcal/mol. Compared with experimental values, the average error for the hydration free energies calculated by the perturbation method for small, neutral molecules is about 1 kcal/mol.²⁴ Larger values may be expected for ionic solutes, as was found with the polarizable continuum model.^{9c} On the other hand, smaller error would be expected for relative values if conformers of a given

molecule are considered. Overall, the deviation found in this study is in accord with the capability of the method.

Relative total free energies presented in Table 3 show large sensitivity to the basis set and the level applied in the calculations. Thus, values in the table should be considered as lower and upper bounds. (By taking the MP2/6-31G* optimized geometries, the calculated ΔG_{sol} value further increases to 2.87 kcal/mol.) Our highest level QCISD(T) calculations using the 6-31G* basis set may reflect the converged value for the T – G1 free energy separation in the gas phase (Table 1). By using this value, the relative free energy of the T conformer in solution was calculated to be 1.64 kcal/mol, which corresponds to a 5–6% fraction in the equilibrium mixture at $T = 296$ K.

The above results indicate that a proper estimate of the quantum mechanical internal energy difference is critical for the present system. If, however, the QCISD(T) estimate is nearly correct, then the solvent effects calculated by Monte Carlo simulations must be overestimated by 1–1.5 kcal/mol, as compared to the experiment. The calculated too large solvent effect may be due to the disregard of the solvent/solute polarization term in the Monte Carlo simulations. In fact, the 12–6–1 OPLS potential does not contain an explicit term for polarization.

Explicit calculation for the polarization term has been performed here within the polarizable continuum model at both the HF/6-31G*//HF/6-31G* and B3LYP/6-31G*//B3LYP/6-31G* levels (Table 3). The values show, however, that the relative term is positive for the T conformer, and thus the inclusion of polarization effects in Monte Carlo simulations would probably even enhance the T – G1 separation. Although the numerical results are very sensitive to the basis set and the method used, interplay between them in the UAHF continuum results predicts, in general, large stabilization of the T conformer

Pair-energy distributions for ion pairs

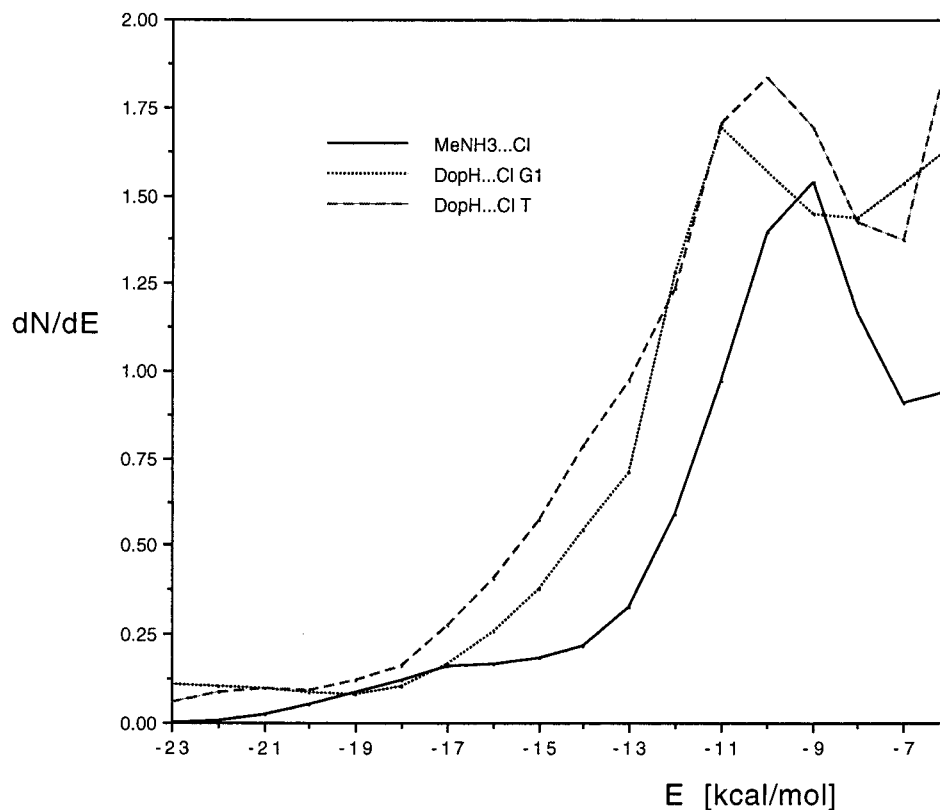


Figure 4. Pair-energy distributions for $\text{MeNH}_3^+\cdots\text{Cl}^-$ ion pair and for the $\text{DopH}^+\cdots\text{Cl}^-$ ion pair with G1 and T conformations for the cation in aqueous solution.

in solution, in contrast to the experiment. The least negative value among those displayed in Table 3, -0.76 kcal/mol, has been obtained for the T – G1 relative free energy in solution by performing MP2/6-31G* calculations^{9d} and considering the fully optimized gas-phase geometries at that level. (All ΔG_{sol} values in the Table, including those calculated by using the PCM method, have been obtained by adding the corresponding thermal correction from Table 1.) This result, associated with a stabilization of G2 with respect to G1, produces a G:T ratio of 50:50. Upon computing the in-solution MP2/6-31G*//HF/6-31G* correlation correction (not indicated), the predicted conformer energies, after the inclusion of thermal corrections are: T – G1 = 0.01 kcal/mol and G2 – G1 = 0.45 kcal/mol, corresponding to a G:T ratio of 60:40. In contrast, at the HF/6-31G*//HF/6-31G* level -1.41 kcal/mol were obtained for the T – G1 relative free energy in solution (0.59 kcal/mol for the G2 – G1 free energy), thus producing a G:T ratio of 11:89. This ratio turned out to be very similar to the B3LYP/6-31G*//B3LYP/6-31G* one, 16:84, derived from T – G1 and G2 – G1 relative energies amounting to -1.50 and -0.23 kcal/mol, respectively.

The polarizable continuum calculations using the UAHF method and parametrization^{9c} probably overemphasize the hydration free energy of the fully exposed trans form by defining too small cavity radii for positive ions (beside other differences in the computational algorithms used). This may be supported either by considering that Alagona and Ghio⁷ found the G1 form as the most stable conformer in solution and relative electrostatic free energies of 0.7 and 0.4 kcal/mol at the HF/6-31G* level for the G2 and T, respectively, when using fixed atomic radii in the original implementation of the polarizable continuum model⁷ or by examining the effect produced when using slightly

Table 4. Coordination Numbers and Number of Hydrogen Bonds for the DopH^+ and MeNH_3^+ Ions with and without Counterion^a

	N/O	H_m/O	H_g/O	H_t/O	Cl/ H_w	N_{HB}	
						$E \leq -10$	$E \leq -8$
T	4.3	1.0	1.0	1.0		2.7	4.4
$T_{\text{HO}\cdots\text{OH}}$	4.5	1.0	1.1	1.1		2.6	4.2
G1	4.2	0.7–1.3	1.0	1.1		2.9	4.2
G2	4.8	undef. ^b	(0.9) ^c	(1.2) ^c		3.1	4.3
MeNH_3^+	4.9		1.3 _{av}			3.6	
T_{counter}	~6	1.1	1.3	1.0	7.5	8.4	11.6
$G1_{\text{counter}}$	~5	1.1	0.5	1.0	7.0	7.5	10.4
$\text{MeNH}_3^+_{\text{counter}}$	4.5		0.9 _{av}		5.8	4.3	7.0

^a H_m is the hydrogen in the meta OH group of dopamine, H_t and H_g are the trans and gauche hydrogens in the NH_3^+ group, respectively, and O and H_w are water atoms. Interaction energy in kcal/mol for calculating N_{HB} , the number of hydrogen bonds. H/O coordination numbers are averaged for MeNH_3^+ . ^b No coordination number was determined because of the poorly defined minimum site of the rdf. ^c A plateau was found between 2.3 and 2.8 Å. A usual limit of 2.5 Å was applied.

larger radii for the NH_3^+ group as compared to those for the CH_2 groups. In the UAHF method, in fact, the radius for NH_3^+ (the H's have no radius per se), fitted during the calculation starting from those obtained from the training set,^{9c} turns out to be exactly equal to the CH_2 ones, although independently fitted. However, the training set contained just $\text{CH}_3\text{--NH}_3^+$ and $\text{C}_6\text{H}_5\text{--NH}_3^+$, where a single conformer dominates the equilibrium population or the conformers differ by methyl rotations only. Therefore, the UAHF method in the present parametrization^{9c} was not tested for conformational problems. By forcing the NH_3^+ radius to be larger by 10, 15, or 20% than the CH_2 ones, we obtained a linear dependence (with regression coef-

N/Ow radial distribution functions

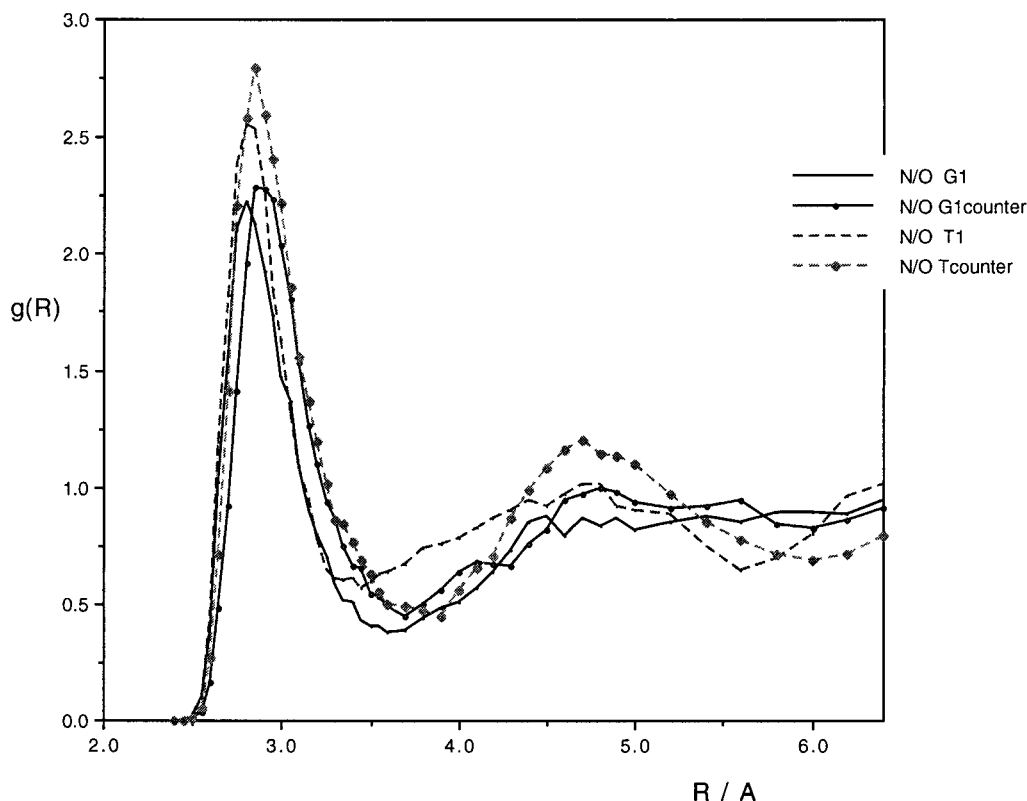


Figure 5. N/O(water) radial distribution functions for the G1 and T conformers of the DopH⁺ ion with and without considering a chloride counterion in the solution.

ficient $r = 0.978$, including the value for the unscaled radius) on the NH₃⁺ radius of the T – G1 relative free energy (–0.63, –0.34, and 0.09 kcal/mol, respectively, at the HF/6-31G*/HF/6-31G* level), whereas the G2 – G1 value turned out to be practically constant. Interestingly, in all of the method/basis set/geometry combinations considered, the use of the scaled NH₃⁺ radius produced a G:T ratio favoring the G forms. At the HF/6-31G*/HF/6-31G* level, the use of an NH₃⁺ radius enlarged by 20% with respect to CH₂ brought the G:T ratio to 61:39. This result is, of course, fortuitous, but it gives an indication that additional efforts are needed to account for conformational preferences in solution.

In all of the calculations reported above it was assumed that the O–H···O–H moiety maintains the internal hydrogen bond. In our previous investigations for systems with such a bonding pattern^{11a,b,12a} free energy perturbation calculations indicated a large stabilization of the H–O···O–H arrangement, thus, when the intramolecular hydrogen bond is disrupted. Monte Carlo simulations for the trans DopH⁺ ion confirmed this hypothesis: the solvation free energy is more negative by 3.96 ± 0.12 kcal/mol for the structure without rather than with an O–H···O internal hydrogen bond. The MP2/6-311++G**/HF/6-31G* internal energy is, however, higher for this structure by 5.91 kcal/mol. The HF/6-31G* value is 6.29 kcal/mol. As a result, the overall free energy effect upon disruption of the internal bond is unfavorable by about 2 kcal/mol in aqueous solution. Accordingly, this less favorable T conformer cannot decrease the previously calculated T – G1 separation.

Thus we can conclude, by applying the approximations used in the present calculations, that the combined ab initio/Monte Carlo method fails to quantitatively predict the T – G1 free energy difference in solution. A key problem in the simulation is the applied charge set, as mentioned above. The lack of a

prediction of a G:T ratio in accord with the experimental value, mainly when using higher level ab initio calculations, may call into question the reliability of the calculated solvent effects. Application of a different charge set, e.g., AM1/CM2, may be useful in a future work.

Nonetheless, present calculations have revealed that the solvent effects are favorable by $(-2.22 \pm 0.31) - 0.41 = -2.63 \pm 0.31$ kcal/mol for the trans as compared to the more stable gauche conformer (Table 3). This finding is consistent with previous calculations for systems with the X–CH₂–CH₂–NH₃⁺ moiety (X = aromatic ring).^{4,6,7,32,34} The G2 – G1 internal free energy difference does not show large basis set and correlation level sensitivity; ΔG_{sol} in Table 3 is in the range of 1.43–1.65 kcal/mol. The range is practically hidden by the standard deviation of 0.43 kcal/mol for the solution calculations. In the absence of experimental data, however, the calculated value has no basis for comparison.

Solution Structure. Figures 3 and 4 show the pair-energy distribution functions for single ions and ion pairs. Integration of the distribution curve for the MeNH₃⁺ ion up to the end of its minimum at –10 kcal/mol defines 3.6 hydrogen bonds with the solvent molecules (N_{HB} in Table 4). Integration of the curves for the dopamine conformers until this limit results in only 2.6–3.1 hydrogen bonds. The gauche DopH⁺ ions have, however, a minimum or an end of a plateau at –8 kcal/mol that is a more appropriate upper limit in this case. By integration up to this limit for the dopamine conformers (including the trans one, as well) a total of 4.2–4.4 hydrogen bonds was obtained. The increased values include contributions from weaker hydrogen bonds to the NH₃⁺ segment and also from hydrogen bonds to the phenolic groups. Indeed, the most negative pair-energy

(34) Worth, G. A.; Richards, W. G. *J. Am. Chem. Soc.* **1994**, *116*, 239.

Hg/O radial distribution functions

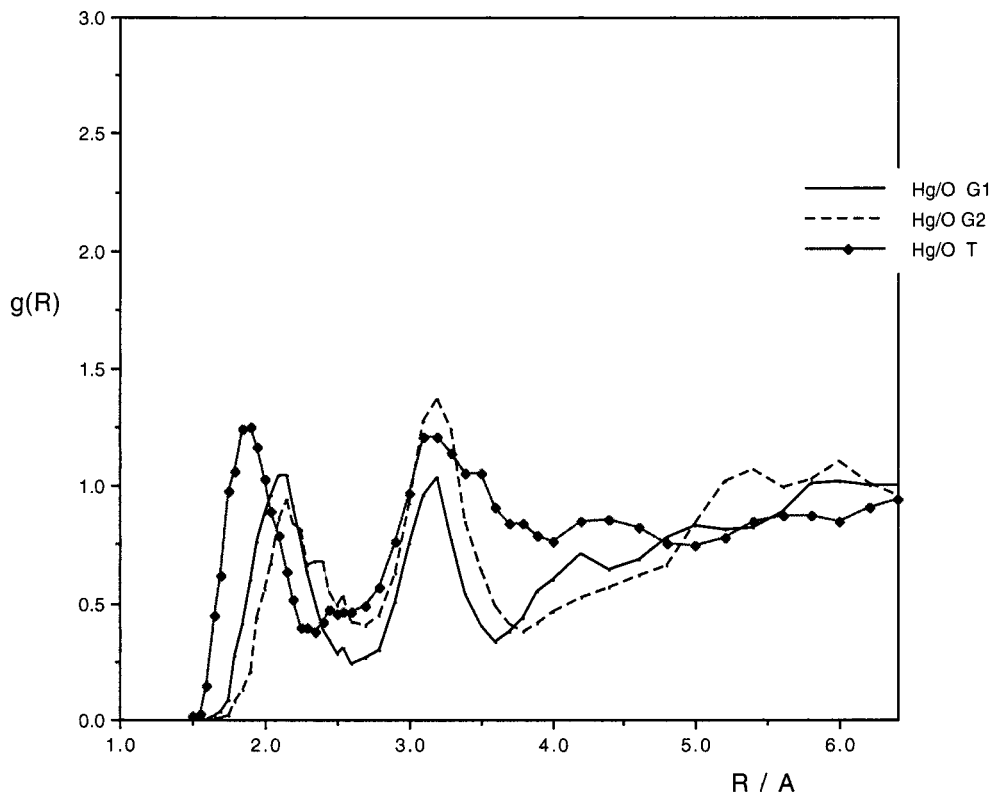


Figure 6. H(gauche in the NH_3 group)/O(water) radial distribution functions for the G1, G2, T conformers of a single DopH^+ ion in aqueous solution.

interactions for the 2-OH benzoic acid^{12a} with an O–H \cdots O–H substructure fall in the -10 to -8 kcal/mol energy range.

Pair-energy distribution functions for ion pairs differ basically from those for single ions (Figure 4). The rise of the curve starts at -22 kcal/mol for $\text{MeNH}_3^+\cdots\text{Cl}^-$ and around -27 kcal/mol for the $\text{DopH}^+\cdots\text{Cl}^-$ systems. Integration up to the most negative E value found for the corresponding single ion (Figure 3) gives 0.3 hydrogen bonds between the solvent and the $\text{MeNH}_3^+\cdots\text{Cl}^-$ ion pair, and ~ 1 hydrogen bond in the case of the $\text{DopH}^+\cdots\text{Cl}^-$ solute. These water molecules must be the most strongly bound ones. The different values for the two systems are reasonable: the $\text{N}\cdots\text{Cl}$ distance is 3.6 Å for the $\text{MeNH}_3^+\cdots\text{Cl}^-$ system and 6 Å for the $\text{DopH}^+\cdots\text{Cl}^-$ ion pair. There is no room for accommodating a water molecule between the N and Cl atoms in the former case. Strongly bound water molecules can only stay away from the line connecting the two reference atoms. In contrast, the 6 Å separation of the $\text{N}\cdots\text{Cl}$ atoms allows one water molecule to be accommodated between the two atoms and to develop a strong N–H \cdots OwHw \cdots Cl interaction, as reflected by the onset value of at least -26 kcal/mol for the pair-energy distribution functions. For the solvent separated $\text{DopH}^+\cdots\text{Cl}^-$ ion pair the N_{HB} value is nearly the sum of the Cl/H_w coordination number and the N_{HB} value for the single ion (at $E \leq -8$): $7.5 + 4.4$ vs 11.6 for T and $7.0 + 4.2$ vs 10.4 for G1 (Table. IV). Thus if the $\text{N}\cdots\text{Cl}$ separation reaches 6 Å, the N–H \cdots O and O–H \cdots Cl hydrogen bonds can be formed without disturbance by the other solute.

Radial distribution functions (rdf's) in Figures 5–8 show fine differences of the solution structure around the protonated dopamine solute. The N/O rdf's (Figure 5) indicate higher (first and second) peak values for the trans rather than for the gauche conformer, and the peak values are higher with than without a

counterion for both conformers. These results mean more localized water molecules around the trans NH_3^+ group as compared to the gauche one. The solute–solvent interaction energy becomes more negative but, in parallel, stronger localization of the solvent molecules reduces the entropy of the system. The overall effect still might be favorable ($\Delta G(\text{solv})$ (T – G1) = -2.22 ± 0.31 kcal/mol), but upon adding a counterion to the system a preferentially stronger localization of the water molecules around the trans conformer (increases in the $g(R)$ curves are remarkable only with the T conformer) results already in a decrease of the solvation preference of the T conformer to a small value of 0.14 kcal/mol, presumably due to entropic effects.

Fine details of the hydration of the N–H bonds can be observed by studying the rdf's in Figures 6–7. The H/O distributions for the gauche hydrogen in the C–C–N–H moiety (Figure 6) show relatively small differences in any conformations. The first peak value of $g(R)$ is the largest for the trans conformer, because the gauche hydrogen, which points rather toward the catechol ring, can be less hydrated because of steric effects.

Figure 7 shows the rdf's for the trans C–C–N–H hydrogen. While the $g(R)$ value for the first H_t/O peak is 1.5 , near the value of 1.25 in the H_g/O curve for the T conformer, the G1 values differ remarkably. The H_g/O and H_t/O peak values are 1 and 2, respectively, indicating that the hydration of the trans hydrogen is much stronger than that of the gauche hydrogen in the G1 conformer. It may be, however, a compensation effect: since the gauche hydrogen is shielded against hydration by the ring, the trans hydrogen exposed to the solvent binds water molecules in an even stronger way than in the T conformation. The counterion decreases the peak value for the T conformer

Ht/O radial distribution functions

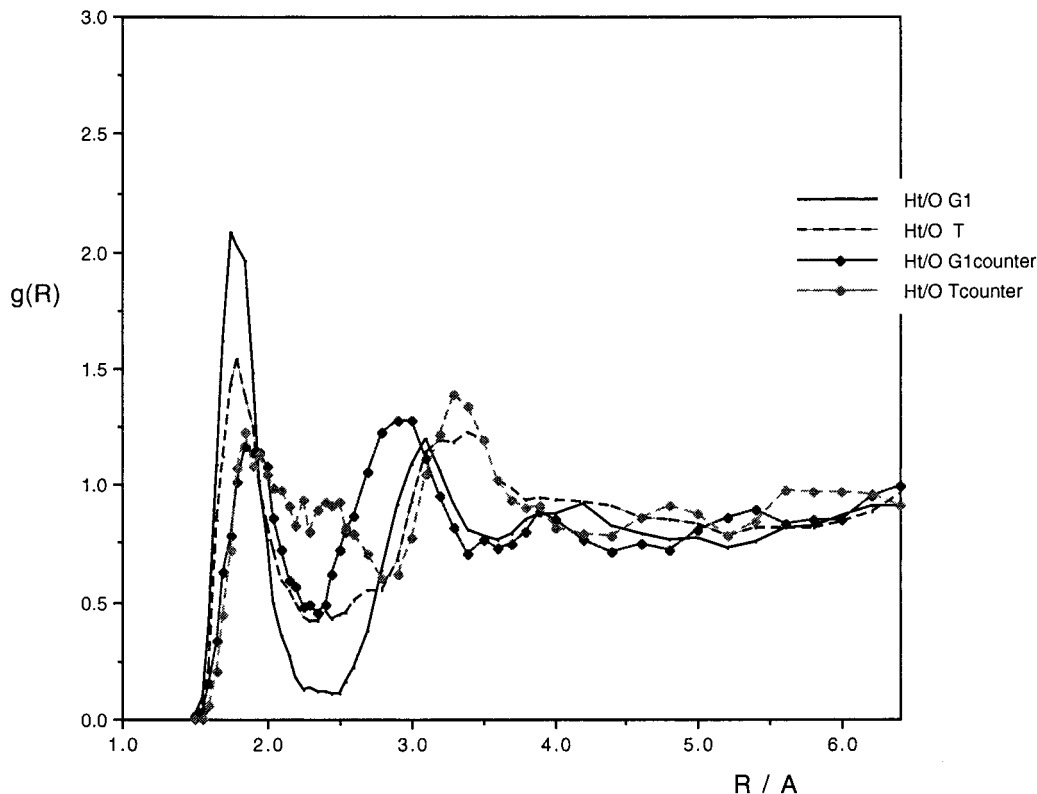


Figure 7. H(trans in the NH_3 group)/O(water) radial distribution functions for the G1 and T conformers of the DopH^+ ion with and without considering a chloride counterion in the solution.

from 1.5 to 1.25, but from 2 to 1.2 for the G1 form. The calculated H_g/O coordination number for $\text{G1}_{\text{counter}}$ is nearly half of the general H/O value in Table 4.

Hydration of the two OH groups shows different dependence on the side chain conformation. In the most stable arrangement with the $\text{O}_m-\text{H}_m\cdots\text{O}_p$ intramolecular hydrogen bond⁷ the para OH is exposed to the solvent, and forms one $\text{O}_p-\text{H}_p\cdots\text{O}_w$ intermolecular hydrogen bond, as calculated from the H_p/O_w coordination number, in every conformation. Hydration of the meta OH is, however, conformation-dependent (Figure 8). The G2 side chain conformation provides fairly strong steric hindrance against hydration of the meta OH (Figure 1). Height of the first peak of the H_m/O rdf is about half that for the T conformer. The $g(R)$ curve does not indicate any preferred localization distance below 3 Å, thus assignment of an H_m/O coordination number for the G2 conformer may not be done without ambiguity. The marked difference between the T and G2 H_m/O rdfs may be attributed to the steric repulsion felt by water molecules from the gauche NH_3^+ group. In contrast to the first, the second and third peaks are structured, but reflecting water oxygens strongly bound to other sites, as the OH_p or NH_3^+ groups.

The first peak of the H_m/O rdf in the T conformer shows only a small shift upon disruption of the intramolecular $\text{O}-\text{H}_m\cdots\text{O}_p-\text{H}$ bridge, indicating no basic change in the $\text{O}_m-\text{H}_m\cdots\text{O}_w$ hydration pattern. Indeed, the intramolecular $\text{O}-\text{H}\cdots\text{O}$ bond is strongly bent (about 110°) and fairly long ($\text{H}\cdots\text{O}$ distance is about 2.2 Å); thus, hydration of the meta H from the side opposite to O_p (in the $\text{O}-\text{H}\cdots\text{O}$ plane) requires only moderate bending and stretching for the $\text{O}_m-\text{H}_m\cdots\text{O}_w$ bond. When the intramolecular hydrogen bond is disrupted ($\text{T}_{\text{disrupt}}$), the meta H can be fully hydrated. The height of the first $g(R)$

peak slightly increases and its R site is shifted toward lower values by about 0.05–0.1 Å.

Conclusions

The protonated dopamine cation exhibits a trans (T) and two gauche (G1 and G2) conformations in the gas phase, distinguished by the positions of the catechol ring and the NH_3^+ cationic head relative to the $\text{C}(\text{ring})-\text{C}_\beta-\text{C}_\alpha$ plane. The OH groups are nearly coplanar with the benzene ring and form either an $\text{O}-\text{H}\cdots\text{O}-\text{H}$ intramolecular hydrogen bond or show an $\text{H}-\text{O}\cdots\text{O}-\text{H}$ disrupted pattern. Each conformer is of C_1 symmetry, thus exists in a mirror-image pair in the equilibrium mixture. Single point ab initio quantum chemical calculations up to the QCISD(T)/6-31G* level and optimization at the MP2/6-311++G** level predict free energy differences of 3.2–5.6 kcal/mol for the T – G1 and about 0 kcal/mol for the G2 – G1 at 298 K and 1 atm. The $\text{O}-\text{H}\cdots\text{O}-\text{H}$ structure is more stable than the disrupted one by about 6 kcal/mol.

Theoretical calculations find one trans and two gauche low-energy conformers in aqueous solution. The T – G1 and G2 – G1 relative solvation free energies, determined by the free energy perturbation method in Monte Carlo simulations and corrected for the long-range electrostatic effects, are -2.63 ± 0.31 and 1.34 ± 0.43 kcal/mol, respectively, at $T = 310$ K. If a chloride counterion is also considered in the system with $\text{N}\cdots\text{Cl}$ separation of 6 Å, the T – G1 relative solvation free energy is reduced to -0.55 ± 0.95 kcal/mol. The calculated total free energy difference for the T and G1 conformers is at least 0.6 ± 0.3 kcal/mol in aqueous solution. The calculated value for the G2 – G1 free energy separation is about 1.5 kcal/mol. The inclusion of the solute polarization free energy, as

Hm/O radial distribution functions

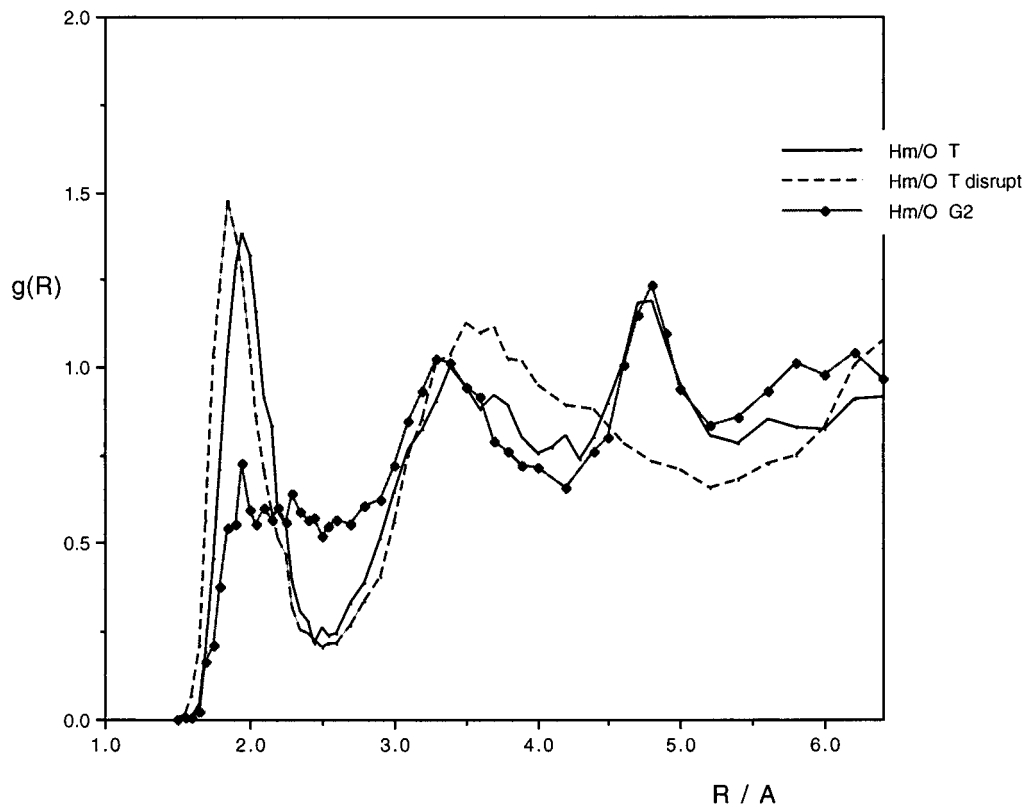


Figure 8. H(meta OH)/O(water) radial distribution functions for the T and G2 conformers of the DopH⁺ ion in aqueous solution. T(disrupt) curve refers to the trans conformer with H—O···O—H arrangement at the catecholic site.

calculated from the polarizable continuum model, would further increase the relative free energy for the T and G2 conformers.

Combined ab initio/Monte Carlo calculations reproduce experimental results qualitatively for the conformational equilibrium. The G1 conformer is the prevailing one in the mixture, but the smallest predicted G:T ratio, 75:25, is larger than 58:42 found for the gauche–trans distribution at pH = 7 and at $T = 296$ K in D₂O. Although the relative internal energy term shows large sensitivity to both the basis set and the level at which electron correlation is considered, the exaggerated G1 fraction is rather attributed to the underestimate of the solvent stabilization for the trans form throughout Monte Carlo simulations. Nonexplicit consideration of the polarization effects and a simple representation of the solution at pH = 7 could lead to a summation instead of cancellation of the modeling errors. Overall preference of the trans form (with the exception of the MP2/6-31G*//HF/6-31G* calculations) by the UAHF polarizable continuum calculations may be attributed to probably too short cavity radii accepted for cations.

When dopamine acts in a real biological system, its protonated form is surrounded, at least for a part of the interaction, by water molecules and counterions, presumably chloride anions. Computer modeling for the upper bound of the counterion effect by considering a single-water separated DopH⁺···Cl⁻ ion pair (by setting the N···Cl distance to 6 Å) shows that the close

counterion largely modifies the solution structure in the immediate vicinity of protonated dopamine. The effect for the gauche conformer is different from that for the trans one, leading to a decrease of the solvation preference for the trans form. Although the single-water separated DopH⁺···Cl⁻ ion pair is not favored in the bulk aqueous solution, such arrangement is possible in more restricted regions, e.g., in a receptor cavity or when passing membranes. In these cases one could expect an increase in the G1 conformer over the T form at pH = 7.4 and $T = 310$ K as compared to the G1:T ratio found in D₂O solution of dopamine at pH = 7.

Acknowledgment. Peter I. Nagy thanks the Ohio Supercomputer Center for the granted computer time used in performing part of the quantum chemical calculations. He also thanks Professor Jorgensen for the use of the BOSS 3.6 software. G.A. and C.G. are grateful to the CNUCE computing center for a grant used to carry out the frequency calculations.

Supporting Information Available: Four figures, S1–S4 showing the changes of ΔE , $\Delta G(\text{gas})$, and ΔG_{sol} (with and without counterion) along the perturbation pathways p1–p4 (PDF). This material is available free of charge via the Internet at <http://pub.acs.org>.

JA981528V